

Pyrochlore-Type Compounds Containing Double Oxides of Trivalent and Tetravalent Ions¹

Robert S. Roth

A study has been made by X-ray diffraction analyses of the $A_2O_3 \cdot 2BO_2$ -type double oxides. It was found that many of these mixed oxides, after appropriate heat treatment, formed compounds of the formula type $A_2B_2O_7$. Most of these compounds crystallized in the cubic system with a face-centered cell similar to that found for the mineral pyrochlore, although some were distorted from the ideal cubic structure.

Indexed X-ray diffraction powder patterns are given for the cubic compounds $Sm_2O_3 \cdot 2TiO_2$, $Gd_2O_3 \cdot 2TiO_2$, $Dy_2O_3 \cdot 2TiO_2$, $Y_2O_3 \cdot 2TiO_2$, $Yb_2O_3 \cdot 2TiO_2$, $La_2O_3 \cdot 2SnO_2$, $Nd_2O_3 \cdot 2SnO_2$, $La_2O_3 \cdot 2ZrO_2$, $Nd_2O_3 \cdot 2ZrO_2$, and for the possible compounds $Y_2O_3 \cdot 2ZrO_2$ and $Nd_2O_3 \cdot 2UO_2$. Unindexed patterns are given for $La_2O_3 \cdot 2TiO_2$, $Nd_2O_3 \cdot 2TiO_2$ and $Bi_2O_3 \cdot 2SnO_2$.

On the basis of the existence of the two compounds $La_2O_3 \cdot 2ZrO_2$ and $Nd_2O_3 \cdot 2ZrO_2$, the phase diagrams for the systems La_2O_3 - ZrO_2 and Nd_2O_3 - ZrO_2 have been revised.

1. Introduction

A partial survey of the reactions occurring in binary oxide mixtures of the type $A_2O_3 \cdot 2BO_2$ has been conducted as part of a program of fundamental research on ceramic materials. Combinations of simple oxides in this proportion were selected because of the current interest in ferroelectric ceramics. $Cd_2Nb_2O_7$, at room temperature, has the cubic pyrochlore structure, although the ferroelectric form at low temperatures is distorted from this ideal structure [1, 2, 3].² The fact that the compound $Cd_2Nb_2O_7$ is known to be ferroelectric at certain temperatures [1] led to the study of other compounds with similar structure.

At the time this work was initiated, no references were known describing a pyrochlore structure that did not contain a pentavalent ion as an essential element of the compound. A ternary compound of this type having the formula $CaO \cdot ZrO_2 \cdot 2TiO_2$ or $(Ca_{1.0}Zr_{1.0})Ti_2O_7$ was, however, described by Coughanour et al. [4]. Another reference has recently been made by Padrow and Schusterius [5] to pyrochlore phases in the system La_2O_3 - SnO_2 - TiO_2 .

This report is concerned with some combinations of the oxides of trivalent and tetravalent ions which, on the basis of radius ratio, might be expected to form compounds of the pyrochlore type.

2. Materials and Methods

2.1. Materials

The following substances were used as sources of the component oxides in this study:

TiO_2 . A rutile of 99.5-percent purity.

SnO_2 . Precipitated tin oxide of over 98.5-percent purity.

ZrO_2 . Dense zirconia of over 99-percent purity, calcined at 1,450° C.

CeO_2 . Calcined cerium dioxide of nominal 99-percent purity.

UO_2 . Urania, supplied by the United States Atomic Energy Commission, of over 99.9-percent purity.

La_2O_3 . Lanthanum oxide of 98-percent purity, remainder mostly water and CO_2 .

Nd_2O_3 . Neodymium oxide of over 99-percent purity.

Sm_2O_3 . Samarium oxide of nominal 99-percent purity.

Gd_2O_3 . Gadolinium oxide of nominal 98-percent purity.

Bi_2O_3 . Bismuth trioxide of over 99-percent purity.

$Bi_2O_3 \cdot 3SnO_2 \cdot 5H_2O$. Precipitated hydrous bismuth stannate of at least 98-percent purity.

Y_2O_3 . Yttrium oxide of 98- to 99-percent purity, the remainder being rare earths.

Dy_2O_3 . Dysprosium oxide of nominal 98-percent purity.

Yb_2O_3 . Ytterbium oxide of nominal 98-percent purity.

In_2O_3 . Rather impure indium oxide specified "for manufacturing use only."

Sb_2O_3 . Antimony trioxide of over 99-percent purity, with 0.2 percent of As_2O_3 .

2.2. Sample Preparation

The starting materials, in sufficient quantities to give either a 10.0-g sample or a 1.0-g sample, depending upon the availability of the raw materials, were weighed to the nearest milligram. No corrections were made for the percentage purity of the raw materials, except for loss due to water and carbon dioxide. They were then mixed together with a few drops of distilled water to assure bonding and formed into 1-in. or ½-in.-diam disks at a pressure of 5,000 lb/in.². The pressed disks were fired for 4 hr at 1,100° C on platinum foil in an air atmosphere, using an electrically heated furnace wound with 80% Pt-20% Rh wire.

¹ This work has been sponsored as part of a program for Improvement of Piezoelectric Ceramics by the Office of Ordnance Research of the Department of the Army.

² Figures in brackets indicate the literature references at the end of this paper.

Following the preliminary heat treatment, the disks were ground, using a mullite mortar and pestle, remixed with a few drops of distilled water, and new disks, about $\frac{1}{4}$ in. high, were formed at 15,000 lb/in.² in either a $\frac{1}{2}$ -in. or $\frac{1}{4}$ -in.-diam mold. These specimens were then ready to be used for solid-state reaction studies. Some of the specimens used were prepared by G. R. Shelton of the Bureau during the last 10 years by methods similar to those described here. Most of these specimens were reheated, in the present study, to obtain better crystallinity.

2.3. Study of Solid-State Reactions

In the study of solid-state reactions, a conventional platinum-wound quench furnace was used. The temperature in the furnace was measured with a Pt versus Pt-10-percent-Rh thermocouple and controlled by a modified Roberts-type controller. The quenching technique was used because it has been observed that sharper X-ray patterns are often obtained by very fast cooling of the specimen. Phase transitions in the pyrochlore structure are probably completely reversible and cannot be "frozen in" by quenching. For quench tests, the $\frac{1}{2}$ - or $\frac{1}{4}$ -in.-diam disks were placed on a platinum platform, which was then suspended in the furnace. The test temperature ranged from 1,250° to 1,550° C and was maintained constant for a given length of time. Equilibrium conditions were usually reached in less than 3 hr. Equilibrium was believed to have been reached when X-ray patterns of the specimen showed only a single phase, or when the pattern of a two-phase specimen showed no change with successive heat treatment. After this reaction time, the sample was quenched in air by lifting the specimen disk on its platinum platform out of the hot furnace. The specimen cooled to room temperature in less than 2 min. The samples were then examined by X-ray diffraction, using a Geiger counter diffractometer employing nickel-filtered copper radiation.

In the case of specimens containing UO₂, an argon atmosphere was used and the specimens were not quenched. The heating element of the furnace used was a molybdenum-wound stabilized ZrO₂ tube and is similar to the one described by Davenport et al. [6].

3. The Pyrochlore-Structure Type

The structure of the mineral pyrochlore and of related mineral types has been described by several workers [3, 7, 8]. Pyrochlore has the formula NaCaNbTaO₆F, in which Na and Ca can be considered the A ions, and Nb and Ta the B ions of an A₂B₂X₇ structure. The space group for this cubic compound has been found to be Fd3m-O_h⁷, with Z=8 and a unit cell of 10.35 to 10.40 Å.

In the following description of the pyrochlore structure, the cell origin has been taken at a center of symmetry and the sets of positions referred to may be found on page 341 of reference [9]. In this structure type there are 16 A ions in position (c), 16 B ions in position (d), and 8 negative ions in

position (a); for the mineral pyrochlore these are the fluorine ions. The remainder of the negative ions (48 oxygen) are in position (f), which contains only one unknown parameter. From a consideration of the spatial requirements in the pyrochlore structure, it is obvious that the value of the unknown parameter must be equal to or very close to $\frac{3}{8}$. If the value of $\frac{3}{8}$ is used, then all possible *xyz* combinations of $\frac{1}{8}$, $\frac{3}{8}$, $\frac{5}{8}$, and $\frac{7}{8}$ are occupied by oxygen, except the eight sites required by the special position (b), which are vacant. In such a structure, if these vacant sites were also occupied, the formula type would be A₂B₂O₈ or ABO₄ instead of A₂B₂O₇. The pyrochlore-structure type may therefore be compared to a fluorite structure with 1 out of every 8 negative ions missing. From data given by Bystrom [3], the value of *x* in the oxygen position for Cd₂Nb₂O₇ and Cd₂Ta₂O₇ can be taken as 0.414 instead of 0.375 for $\frac{3}{8}$. It will be seen in the following discussions that the value of *x* is probably not the same for all of the pyrochlore-type compounds.

In addition to the extinctions to be expected from a face-centered cell, there are two special extinction rules due to the particular positions of the ions in the pyrochlore-type structure:

(1) The positions (a) and (f), filled by negative ions, are such that possible reflections are limited to the type *hkl* where $h+k+l=2n+1$ or $4n$.

(2) The positions (c) and (d), filled by positive ions, are such that possible reflections are limited to planes of the type

$$\left. \begin{array}{l} hkl:h=2n+1 \\ k=2n+1 \\ l=2n+1 \end{array} \right\} \text{ or } \left. \begin{array}{l} 4n+2 \\ 4n+2 \\ 4n+2 \end{array} \right\} \text{ or } \left. \begin{array}{l} 4n \\ 4n \\ 4n \end{array} \right\} .$$

The result is that, in the pyrochlore-type diffraction patterns, certain reflections are always absent. Of those that may be observed, some are due only to metal atom scattering, some only to oxygen atom scattering, and the remainder to both metal and oxygen scattering. Therefore, the intensities of the peaks in the X-ray powder diffraction patterns are characteristic of the pyrochlore structure, and are evidence for the existence of such a structure. Intensity calculations have been made for some of the cubic compounds studied and will be discussed in later sections.

4. Results and Discussion

4.1. General

The X-ray diffraction powder patterns prepared in this study revealed that many of the mixtures formed binary compounds of the type A₂B₂O₇. The great majority of the compounds were cubic, essentially isostructural with the mineral pyrochlore. Table 1 lists the indexed X-ray diffraction powder patterns for these cubic compounds. All of the *hkl*

TABLE 2. Heat treatment and structure type of compositions studied

Composition	Radius ^a of A ⁺³	Radius ^a of B ⁺⁴	Heat treatment ^b		Structure type	Symmetry	Parameter "a"
			Temperature	Time			
La ₂ Ti ₂ O ₇ -----	1.14	0.68	° C	hr	Distorted pyrochlore-----	Unknown-----	-----
Nd ₂ Ti ₂ O ₇ -----	1.04	.68	1,550	1	do-----	do-----	-----
Sn ₂ Ti ₂ O ₇ -----	1.00	.68	1,550	1/2	Pyrochlore-----	Cubic-----	10.228
Gd ₂ Ti ₂ O ₇ -----	0.97	.68	1,550	2	do-----	do-----	10.181
Dy ₂ Ti ₂ O ₇ -----	.92	.68	1,425	1	do-----	do-----	10.106
Y ₂ Ti ₂ O ₇ -----	.92	.68	1,525	1/2	do-----	do-----	10.093
Yb ₂ Ti ₂ O ₇ -----	.86	.68	1,550	2	do-----	do-----	10.030
Im ₂ O ₃ ·2TiO ₂ -----	.81	.68	1,550	3	No compound-----	-----	-----
Sb ₂ O ₃ ·2TiO ₂ -----	.76	.68	1,475	2	do-----	-----	-----
La ₂ Sn ₂ O ₇ -----	1.14	.71	1,550	1	Pyrochlore-----	Cubic-----	10.702
Nd ₂ Sn ₂ O ₇ -----	1.04	.71	1,550	1	do-----	do-----	10.568
Bi ₂ Sn ₂ O ₇ -----	0.96	.71	1,250	1	Distorted pyrochlore-----	Unknown-----	-----
La ₂ Zr ₂ O ₇ -----	1.14	.79	1,550	3	Pyrochlore-----	Cubic-----	10.793
Nd ₂ Zr ₂ O ₇ -----	1.04	.79	1,550	2	do-----	do-----	10.648
Y ₂ Zr ₂ O ₇ -----	0.92	.79	1,550	2	do (?)-----	do-----	10.402(?)
Im ₂ O ₃ ·2ZrO ₂ -----	.81	.79	1,550	3	No compound-----	-----	-----
Im ₂ O ₃ ·2CeO ₂ -----	.81	.94	1,350	1/2	do-----	-----	-----
Nd ₂ O ₃ ·2UO ₂ -----	1.04	.97	° 1,600	1	Fluorite solid solution (?)-----	Cubic-----	5.449
Y ₂ O ₃ ·2UO ₂ -----	0.92	.97	° 1,600	1	No compound-----	-----	-----

^a Radius of the ions taken from Green [10].

^b All specimens, unless otherwise stated, were quenched from the designated temperature.

^c These specimens were heated in an argon atmosphere to prevent the oxidation of UO₂ and were not quenched.

values allowed by a face-centered lattice have been listed, up to and including $h^2+k^2+l^2=192$. It may be seen that none of the peaks forbidden by the structural arrangement of the pyrochlore type are observed in the X-ray patterns of any of the compounds studied.

Table 2 lists the lattice parameters of these compounds, together with the composition, heat treatment, and structure identification for all the materials examined. All compounds and mixtures studied have been plotted in figure 1 on the basis of constituent ionic radii. The values for the radii of the ions have been taken from Green's Geochemical Table of the Elements [10]. The radius of the A⁺³ ion is plotted as the ordinate and that of the B⁺⁴ ion as the abscissa. It can be seen that only the larger A ions with the smaller B ions (the upper left of the

diagram) form compounds. In the lower-right portion of the diagram no compounds are indicated. Thus, areas of compound formation and also of symmetry types can be located on this diagram. This is similar to the types of diagrams given by Wood [11] and by Keith and Roy [12] for perovskite structures. Detailed discussion of each of the compounds studied is given in the following sections.

4.2. Titanates

Most of the rare-earth titanates form compounds having the cubic pyrochlore structure; however, La₂Ti₂O₇ and Nd₂Ti₂O₇ are not cubic. The X-ray diffraction powder data for these two compounds are listed in table 3. The X-ray pattern for La₂Ti₂O₇ is very sharp and clear; however, that of Nd₂Ti₂O₇ is rather diffuse. These compounds seem to be approximately isostructural with CaZrTi₂O₇ [4]. The X-ray patterns of these compounds all have diffraction peaks more or less grouped around the positions that would be expected for a cubic pyrochlore structure. An effort has been made to correlate the structure of these titanates with the orthorhombic form of the A₂B₂X₇ compounds exemplified by the mineral weberite, as described by Bystrom [7] for Ca₂Sb₂O₇ and other antimonates. The titanates reported in the present study do not seem to have the same structure as that reported for the compounds studied by Bystrom, and the X-ray patterns strongly suggest distortions of the pyrochlore type.

The other four rare-earth titanates studied here have the cubic pyrochlore structure, as does yttrium titanate (table 1). These compounds all give very sharp X-ray patterns, with relatively strong additional lines for the hkl peaks required by the pyrochlore structure as compared to the fluorite structure.

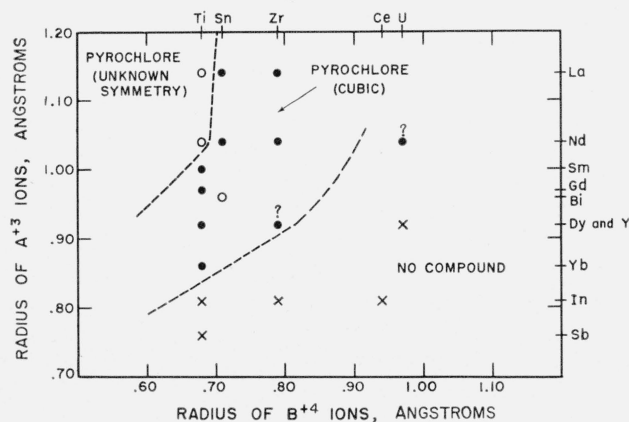


FIGURE 1. Classification of A⁺³B⁺⁴₂O₇ compounds according to the constituent ionic radii.

- Pyrochlore (unknown symmetry).
- Pyrochlore (cubic).
- ⊙ Single-phase face-centered cubic.
- × No compound.

TABLE 3. X-ray diffraction powder data for the compounds $\text{La}_2\text{O}_3 \cdot 2\text{TiO}_2$ and $\text{Nd}_2\text{O}_3 \cdot 2\text{TiO}_2$

$\text{La}_2\text{O}_3 \cdot 2\text{TiO}_2$			$\text{Nd}_2\text{O}_3 \cdot 2\text{TiO}_2$		
2θ	d	I^a	2θ	d	I^a
13.75	6.4	20	13.79	6.4	9
17.37	5.10	6	-----	-----	-----
21.14	4.20	43	21.35	4.16	39
23.00	3.86	12	23.43	3.79	11
β24.98	3.56	5	-----	-----	-----
26.24	3.39	13	26.40	3.37	9
27.70	3.22	b 100++	27.73	3.21	48
28.11	3.17	33	28.61	3.12	25
28.64	3.11	14	29.01	3.07	15
29.79	3.00	b 100+	30.26	2.95	100
32.16	2.78	71	32.30	2.77	30
32.24	2.77	70	32.76	2.73	35
32.96	2.72	71	33.42	2.68	49
33.43	2.68	35	33.75	2.65	21
34.82	2.57	9	35.10	2.55	5
-----	-----	-----	35.95	2.50	6
37.24	2.41	5	-----	-----	-----
38.53	2.33	8	38.65	2.33	9
38.97	2.31	7	39.90	2.26	5
39.96	2.25	30	40.65	2.218	22
41.23	2.188	7	41.92	2.153	10
42.09	2.145	39	42.15	2.142	11
42.36	2.132	25	42.77	2.112	13
43.01	2.101	36	43.45	2.081	26
43.64	2.072	26	44.28	2.044	15
45.14	2.007	15	45.40	1.996	16
45.29	2.001	20	47.32	1.919	31
46.38	1.956	47	47.73	1.904	20
47.12	1.927	31	48.55	1.873	23
48.16	1.888	48	-----	-----	-----
49.54	1.838	8	49.55	1.838	7
49.68	1.833	7	52.12	1.753	15
51.52	1.772	24	52.37	1.745	15
51.68	1.767	21	-----	-----	-----
52.40	1.745	10	54.35	1.686	11
54.00	1.697	15	54.76	1.675	11
54.47	1.683	13	55.72	1.648	15
54.90	1.671	32	56.90	1.617	11
56.00	1.641	17	-----	-----	-----
57.59	1.599	33	58.80	1.569	24
57.98	1.589	25	60.04	1.539	8
58.72	1.571	8	61.62	1.504	10
59.81	1.545	18	62.80	1.478	9
61.26	1.512	16	64.49	1.444	6
62.26	1.490	12	65.21	1.429	6
64.44	1.445	10	66.14	1.412	13
65.14	1.431	26	67.69	1.383	7
66.85	1.398	7	68.62	1.366	6
67.50	1.386	8	69.08	1.358	9
67.92	1.379	9	-----	-----	-----
68.59	1.367	12	70.14	1.341	7
69.10	1.358	10	73.02	1.295	5
70.30	1.338	4	73.55	1.287	5
71.70	1.315	4	74.26	1.276	5
72.50	1.303	5	75.05	1.264	7
73.18	1.292	3	-----	-----	-----
73.55	1.286	14	77.25	1.234	8
73.84	1.282	12	77.50	1.231	7
74.15	1.277	10	78.94	1.212	5
74.43	1.273	9	-----	-----	-----
75.76	1.255	9	79.66	1.203	6
76.28	1.247	5	82.00	1.174	6
76.80	1.240	5	82.28	1.171	6
77.40	1.232	9	83.59	1.156	6
77.64	1.229	8	85.05	1.139	5
78.26	1.221	5	87.49	1.114	5
78.90	1.212	10	87.90	1.110	6
80.10	1.197	4	-----	-----	-----
80.80	1.188	4	88.90	1.100	4
81.65	1.178	4	91.51	1.075	6
82.47	1.168	6	91.80	1.073	6
82.65	1.166	7	-----	-----	-----
85.15	1.138	3	-----	-----	-----
85.83	1.131	8	-----	-----	-----
86.26	1.127	8	-----	-----	-----
86.57	1.123	7	-----	-----	-----
87.37	1.115	5	-----	-----	-----
89.87	1.090	5	-----	-----	-----
90.15	1.088	4	-----	-----	-----

TABLE 3. X-ray diffraction powder data for the compounds $\text{La}_2\text{O}_3 \cdot 2\text{TiO}_2$ and $\text{Nd}_2\text{O}_3 \cdot 2\text{TiO}_2$ —Continued

$\text{La}_2\text{O}_3 \cdot 2\text{TiO}_2$			$\text{Nd}_2\text{O}_3 \cdot 2\text{TiO}_2$		
2θ	d	I^a	2θ	d	I^a
91.25	1.078	5	-----	-----	-----
91.57	1.075	7	-----	-----	-----
92.50	1.066	9	94.06	1.053	6
93.69	1.056	13	95.57	1.040	7
-----	-----	-----	96.72	1.031	6
95.13	1.044	5	97.20	1.027	7
96.15	1.035	7	97.82	1.022	6
98.04	1.020	4	-----	-----	-----
98.98	1.013	3	100.70	1.000	5
100.45	1.002	6	103.12	0.9834	5
100.83	0.9995	5	106.02	.9643	4
103.96	.9777	5	106.60	.9607	7
104.88	.9717	3	107.70	.9539	5
105.22	.9694	4	110.79	.9358	4
108.40	.9497	4	-----	-----	-----
110.25	.9388	9	112.13	.9284	5
111.93	.9294	6	-----	-----	-----
113.31	.9221	7	116.45	.9061	7
113.84	.9192	8	116.87	.9040	2
-----	-----	-----	119.03	.8938	5
-----	-----	-----	120.40	.8876	6
120.70	.8863	7	124.02	.8723	6
123.15	.8758	4	-----	-----	-----
124.08	.8720	4	-----	-----	-----
124.68	.8696	4	-----	-----	-----
125.32	.8671	4	-----	-----	-----
128.35	.8557	3	-----	-----	-----
128.81	.8540	3	-----	-----	-----
130.14	.8494	5	-----	-----	-----
130.82	.8471	5	-----	-----	-----
133.35	.8388	8	139.41	.8212	6
135.10	.8334	5	-----	-----	-----
135.80	.8313	6	-----	-----	-----
137.80	.8256	4	149.87	.7976	5
147.10	.8031	6	-----	-----	-----
148.02	.8012	5	-----	-----	-----
149.92	.7976	5	-----	-----	-----
150.45	.7966	8	158.45	.7841	6
151.65	.7944	7	-----	-----	-----
152.90	.7923	5	-----	-----	-----

^a I is the observed height of the diffraction peaks.
^b These peaks were too strong to be completely recorded on the X-ray pattern.

Table 4 shows the intensity values calculated for a few representative planes of $\text{Sm}_2\text{Ti}_2\text{O}_7$ and other compounds. The intensity values were calculated, using the formula

$$I_{\text{calc.}} \approx F^2 \rho \frac{1 + \cos^2 2\theta}{\sin^2 \theta \cdot \cos \theta}$$

where

F = the structure amplitude as given in reference [9, p. 519].

ρ = multiplicity factor, and the balance of the equation refers to the polarization and Lorenz factors for powder patterns.

These intensities were then recalculated on the basis of 100 for the strongest peak. Table 4 shows the individual contribution of the ions in the structure and the final intensity values compared with the measured peak heights. It can be seen that both the 0.375 value and the 0.414 value of the x parameter for 48 oxygen give poor agreement between observed peak heights and calculated intensity for $\text{Sm}_2\text{Ti}_2\text{O}_7$ although the agreement of the zirconates and stannates is fair for 0.414. It must be concluded that the oxygen parameter for the titanate compounds is slightly different than that reported by Bystrom [3] for the niobates and tantalates.

TABLE 4. Calculated versus observed intensities for some of the diffraction peaks of typical $A_2^{+3} B_2^{+4} O_7$ compounds

hkl	$f \times 16$ A ⁺	$f \times 16$ B ⁺	$f \times 8 O$	$f \times 48 O$		Calculated I^a		Observed I^a
				$x=0.375$	$x=0.414$	$x=0.375$	$x=0.414$	
Sm ₂ Ti ₂ O ₇								
111	-445	126	-48	0	70	50.6	33.1	22
222	829	242	0	0	0	100.0	100.0	b 100+
400	805	232	-22	-269	-150	26.1	35.1	60
331	392	-112	30	0	66	9.6	21.7	36
511/333	-720	589	52	0	31	0.9	0.3	14
Nd ₂ Zr ₂ O ₇								
111	-432	273	-48	0	70	10.5	4.6	5
222	814	514	0	0	0	100.0	100.0	b 100+
400	786	501	-23	-274	-153	26.7	33.6	48
331	384	-245	31	0	68	1.2	5.8	8
511/333	-725	458	53	0	31	4.1	3.0	5
Y ₂ Zr ₂ O ₇								
111	-271	274	-48	0	70	0.9	0.3	0
222	499	512	0	0	0	100.0	100.0	b 100+
400	482	496	-23	-274	-153	24.6	34.1	73
331	238	-246	31	0	68	0.1	1.5	0
511/333	-442	454	53	0	31	.2	0.8	0
Nd ₂ Sn ₂ O ₇								
111	-432	350	-48	0	70	3.3	0.9	4
222	811	661	0	0	0	100.0	100.0	b 100+
400	782	642	-23	-274	-153	31.5	38.6	77
331	382	-313	31	0	68	0.8	2.2	7
511/333	-720	589	53	0	31	.4	0.2	3

^a I is the height of the diffraction peaks.

^b These peaks were too strong to be completely recorded on the X-ray pattern.

Neither indium nor antimony oxides form compounds with titania. The X-ray patterns for the mixtures $In_2O_3 \cdot 2TiO_2$ and $Sb_2O_3 \cdot 2TiO_2$ show only the presence of TiO_2 . The specimens had contracted and lost weight, indicating that the other oxide had volatilized and had not combined with titania. It was found that, if In_2O_3 or Sb_2O_3 reacts with a second oxide to yield a true compound, little or no material is lost in volatilization under the heating conditions used in these experiments.

4.3. Stannates

Both of the rare-earth oxides, lanthana and neodymia, form cubic compounds with stannic oxide. There are only a few small peaks in the X-ray diffraction powder patterns (table 1) that cannot be indexed on the basis of a fluorite-type structure with a unit-cell size of approximately 5 Å. However, these additional lines indicate that the true structure is that of the pyrochlore type with a cell size of approximately 10 Å. The diminished intensity of these excess lines, as compared to those of the titanates, is due to the small difference in the scattering power of the two metal ions, as shown in table 4 for $Nd_2Sn_2O_7$. No other rare-earth stannates have been studied, but it is probable that many of them form cubic pyrochlore compounds. Also, it is evident, from the work of Padrow and Schusterius [5] that solid solutions of the rare-earth titanates and stannates can occur.

TABLE 5. X-ray powder diffraction data for the compound $Bi_2O_3 \cdot 2SnO_2$

d	I^a	d	I^a	d	I^a
6.2	25	1.496	7	1.028	15
3.77	14	1.428	5	1.006	4
3.61	46	1.425	6	0.9964	4
3.22	27	1.419	10	.9924	4
3.08	b 100++++	1.394	7	.9814	3
2.78	21	1.391	9	.9756	3
2.67	b 100++++	1.372	4	.9641	4
2.47	15	1.349	8	.9446	5
2.45	22	1.336	17	.9338	6
2.39	8	1.328	6	.9315	5
2.35	13	1.296	6	.9277	5
2.240	10	1.259	4	.9200	4
2.181	5	1.253	8	.9168	4
2.090	5	1.235	7	.9067	6
2.065	7	1.226	30	.9033	14
2.057	11	1.205	9	.8905	9
1.998	6	1.195	25	.8817	4
1.888	b 100+++	1.175	7	.8765	4
1.868	8	1.173	7	.8705	4
1.812	21	1.166	6	.8645	5
1.807	16	1.161	5	.8584	5
1.780	11	1.148	6	.8480	6
1.763	14	1.139	4	.8449	8
1.717	16	1.122	5	.8374	5
1.690	8	1.110	6	.8346	5
1.629	9	1.091	15	.8242	3
1.610	b 100+	1.075	5	.8171	8
1.597	12	1.054	4	.8149	7
1.542	32	1.045	4	.8054	6
1.531	13	1.033	9	.7987	8

^a I is the observed height of the diffraction peaks.

^b These peaks were too strong to be completely recorded on the X-ray pattern.

The reaction between Bi_2O_3 and SnO_2 has been studied extensively by Coffeen [13, 14], who indicated that the hydrous bismuth stannate, $Bi_2(SnO_3)_3 \cdot 5H_2O$, fired at 1,149° C, formed the compound $Bi_2(SnO_3)_3$. The present study indicates that the $Bi_2O_3 : 3SnO_2$ mixture contains a new compound plus free SnO_2 , and that the composition $Bi_2O_3 \cdot 2SnO_2$ contains no free SnO_2 . It had been reported by Aurivillius [15] that the system $Bi_2O_3 - TiO_2$ contained a compound, $Bi_4Ti_3O_{12}$, that was pseudotetragonal, actually orthorhombic; therefore, the analogous compound $2Bi_2O_3 : 3SnO_2$ was looked for in the $Bi_2O_3 - SnO_2$ system. The reported structure could not be correlated with the compound found in the $Bi_2O_3 - SnO_2$ system. It must therefore be concluded that the $Bi_2O_3 - SnO_2$ compound is not isostructural with $Bi_4Ti_3O_{12}$, but has a distorted pyrochlore-type structure with a ratio of $Bi_2O_3 : 2SnO_2$.

The X-ray pattern of the $Bi_2O_3 \cdot 2SnO_2$ compound given in table 5 resembles very strongly those of the cubic pyrochlores. All of the cubic peaks for a 10.68 Å cubic pyrochlore structure can be found in this pattern, although there are other peaks present. A cubic unit cell of 21.37 Å could account for most of these excess peaks, but some would be still unexplained. Although the pattern is very strongly pseudo-cubic, it must be concluded that the true symmetry is other than cubic.

It may be seen in figure 1 that the radius of the Bi^{+3} ion is close to that of Gd^{+3} and, on the basis of radius ratio only, could be expected to form a cubic pyrochlore structure with SnO_2 . However, the electronic polarization of the Bi^{+3} ion is probably different from that of the rare earths and may be

related to the distortion from cubic symmetry. This notion of electronic polarization has been very valuable in explaining the distortion from cubic symmetry in the perovskite structures [16].

4.4. Zirconates

Specimens of $\text{La}_2\text{O}_3 \cdot 2\text{ZrO}_2$ and $\text{Nd}_2\text{O}_3 \cdot 2\text{ZrO}_2$ were carefully examined by X-ray diffraction powder analysis because previous work by Brown and Duwez [17] indicated that no compounds existed in these two systems. Table 1 shows that several extra lines of relatively low intensity were found in both patterns, which could be indexed only on the basis of a cubic pyrochlore-type compound. In table 4 the intensities calculated for $\text{Nd}_2\text{Zr}_2\text{O}_7$, using an oxygen parameter of 0.414, agree very well with the observed peak heights. A compound at a composition of $\text{La}_2\text{O}_3 \cdot 2\text{ZrO}_2$ was suggested by Trombe and Foex [18]. From the data presented it must be concluded that the compounds $\text{La}_2\text{Zr}_2\text{O}_7$ and $\text{Nd}_2\text{Zr}_2\text{O}_7$ do indeed exist and probably have a wide solid-solution range. They would fall in the middle of the stabilized cubic zirconia solid-solution regions, shown in the phase diagrams of the systems $\text{La}_2\text{O}_3\text{-ZrO}_2$ and $\text{Nd}_2\text{O}_3\text{-ZrO}_2$, proposed by Brown and Duwez [17] and reproduced here as figures 2 (a) and 3 (a). These compounds are indicated in the proposed revision of the two phase diagrams, figures 2 (b) and (c), and 3 (b). The compounds $\text{La}_2\text{O}_3 \cdot 2\text{ZrO}_2$ and $\text{Nd}_2\text{O}_3 \cdot 2\text{ZrO}_2$ have been indicated as melting congruently in figures 2 (b) and 3 (b) for the purpose of simplicity of the phase diagram, although no information is available on

the melting points. If the compound melted incongruently, there could be no field of $\text{La}_2\text{Zr}_2\text{O}_7$ (or $\text{Nd}_2\text{Zr}_2\text{O}_7$) solid solution on the high ZrO_2 side of the compound. This would not agree with the observed widening of the single-phase cubic solid-solution area shown by Brown and Duwez [17]. Figure 2 (c) indicates the phase equilibria in the $\text{La}_2\text{O}_3\text{-ZrO}_2$ system if the pyrochlore compound actually melted incongruently.

It might be thought possible to have both a compound and a cubic ZrO_2 solid solution in the phase diagrams. Such a situation would demand that the diffraction peaks in the X-ray patterns of the fluorite-type solid-solution phases coincided with the strong peaks of the pyrochlore compound, so as to agree with the observed single-phase solid solution. A highly complex diagram of this sort could be drawn for either a congruently or an incongruently melting compound. As a complexity of such a nature is unlikely, it is thought that the phase diagrams, figures 2 (b) and 3 (b), best fit all of the observed data.

It has been claimed by Ruff and Ebert [19], and Duwez, Brown, and Odel [20] that Sc_2O_3 , Sm_2O_3 , Gd_2O_3 , and Y_2O_3 all form cubic zirconia solid solutions. These conclusions have been quoted by Dietzel and Tober [21]. In the present study, only the $\text{Y}_2\text{O}_3 \cdot 2\text{ZrO}_2$ composition has been examined. This specimen is apparently that of a single-phase fluorite material with no additional lines observable.

It is possible that the $\text{Y}_2\text{O}_3 \cdot 2\text{ZrO}_2$ composition is a true pyrochlore compound in which the faint

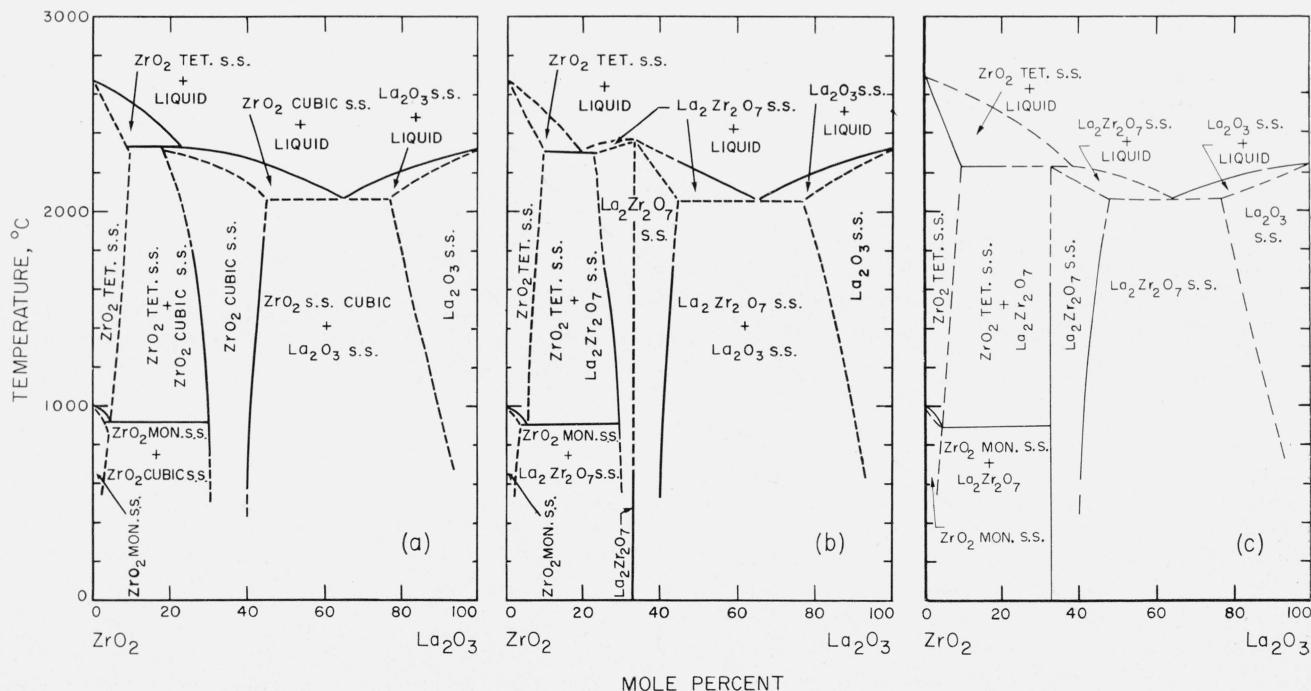


FIGURE 2. Possible phase equilibria in lanthana-zirconia system.

(a) Phase equilibria in the system lanthana-zirconia according to Brown and Duwez [17]. (b) Postulated phase equilibria in the system lanthana-zirconia showing the compound $\text{La}_2\text{Zr}_2\text{O}_7$ melting congruently with solid solution on both sides of the compound. (c) Possible phase equilibria in the system lanthana-zirconia showing the compound $\text{La}_2\text{Zr}_2\text{O}_7$ melting incongruently with solid solution only on the high La_2O_3 side of the compound.

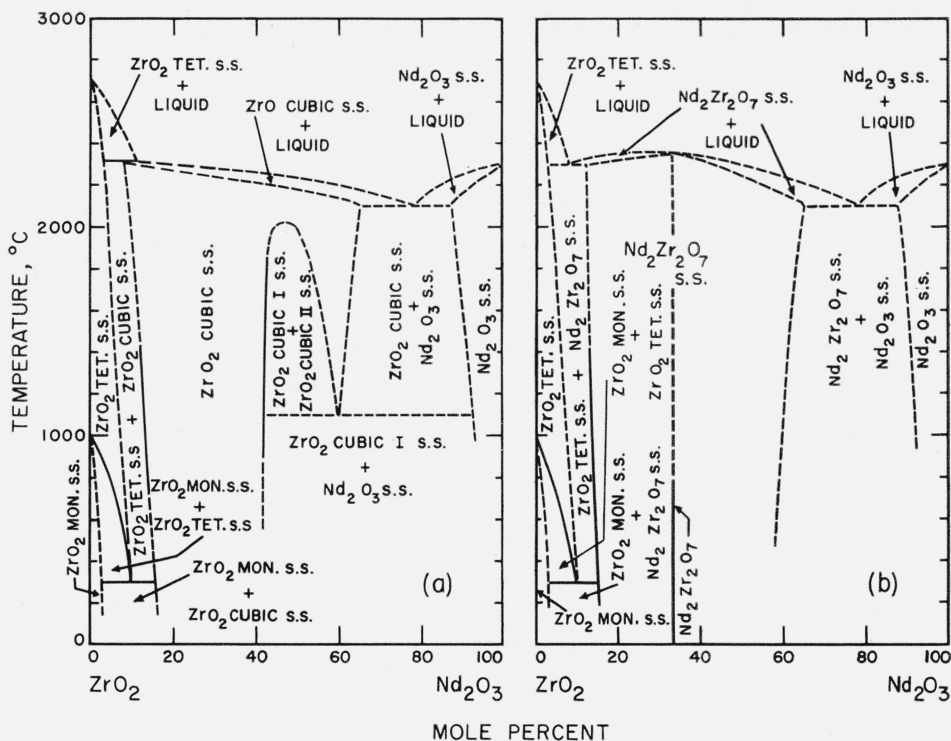


FIGURE 3. Possible phase equilibria in the neodymia-zirconia system.

(a) Phase equilibria in the system neodymia-zirconia according to Brown and Duwez [17]. (b) Postulated phase equilibria in the system neodymia-zirconia showing the compound $\text{Nd}_2\text{Zr}_2\text{O}_7$ melting congruently with solid solution on both sides of the compound.

lines characteristic of pyrochlore are too weak to be observed. As shown in table 4, the intensity of these lines is almost entirely due to the difference in the scattering power of the A and B ions. The relative intensity of the additional peaks should be very small as the scattering factors of Y^{+3} and Zr^{+4} are almost exactly equal and the intensities depend almost entirely on the oxygen ions. The observed peak heights and the calculated intensities of $\text{Y}_2\text{Zr}_2\text{O}_7$ show good correlation. Although it cannot be unequivocally decided whether the $\text{Y}_2\text{O}_3:2\text{ZrO}_2$ composition is a fluorite solid solution or a pyrochlore-type compound, the latter is more probable, and it is not surprising that the excess lines cannot be seen on the X-ray diffraction powder patterns. It is, therefore, proposed that no stabilized cubic ZrO_2 solid solutions exist in mixtures of ZrO_2 and the larger trivalent ions. All such reported occurrences would then be solid solutions of $\text{A}_2\text{B}_2\text{O}_7$ pyrochlore compounds, as shown in figures 2 (b) and 3 (b).

The $\text{In}_2\text{O}_3:2\text{ZrO}_2$ composition also shows only a single cubic fluorite-type phase in the X-ray diffraction powder pattern. As the $\text{In}_2\text{O}_3\text{-ZrO}_2$ system is known to contain two phases in this area [22], and the present specimen contracted considerably and lost weight, it is assumed that the excess In_2O_3 was volatilized and that a cubic ZrO_2 solid solution was actually found in this case.

A general rule can now be given for the reaction of ZrO_2 with various oxides of trivalent metals:

Solid-state reactions of ZrO_2 with oxides of the smaller trivalent ions, for example In_2O_3 , yield cubic ZrO_2 solid solutions; however, the larger trivalent ions probably result in $\text{A}_2\text{B}_2\text{O}_7$ pyrochlore-type solid solutions.

4.5. Cerates and Uranates

a. Cerates

The only cerate composition examined in this study was $\text{In}_2\text{O}_3:2\text{CeO}_2$. The X-ray pattern showed only CeO_2 with no solid-solution or compound formation. The In_2O_3 was believed to have volatilized.

b. Uranates

Only two compositions containing UO_2 , applicable to the present work, $\text{Nd}_2\text{O}_3:2\text{UO}_2$ and $\text{Y}_2\text{O}_3:2\text{UO}_2$, were examined. These preparations have been described elsewhere [23] and will be reviewed briefly here. The $\text{Y}_2\text{O}_3:2\text{UO}_2$ composition was definitely two phases, showing partial solid solution of both components. The X-ray pattern of the $\text{Nd}_2\text{O}_3:2\text{UO}_2$ composition showed a single phase, apparently a fluorite-type solid solution (table 1). In this case the characteristic lines of the pyrochlore structure should easily have been observed, as Nd

has an atomic number of 60, whereas U is 92. When the oxygen positions were shifted considerably from those of the other pyrochlores in an attempt to account for the zero intensity of the additional peaks, improbable uranium to oxygen bond lengths resulted. It must be concluded, therefore, that a compound of the type $\text{Nd}_2\text{U}_2\text{O}_7$ probably does not exist and that the composition $\text{Nd}_2\text{O}_3 \cdot 2\text{UO}_2$ is a single-phase fluorite-type solid solution with an oxygen deficiency.

5. Summary

X-ray diffraction powder data have been presented to show that many $\text{A}_2\text{O}_3 \cdot 2\text{BO}_2$ compositions yield pyrochlore-type compounds when heated to the appropriate temperatures to give solid-state reactions. Oxides of the largest A^{+3} ions with TiO_2 give distorted pyrochlore structures, whereas most of the oxides of the large A^{+3} ions form cubic pyrochlore compounds with the tetravalent ions. Oxides of the smaller A^{+3} ions do not form compounds. This information is shown in a plot of the radius of the A^{+3} ions versus that of the B^{+4} ions. Here it can be seen that certain areas of this diagram enclose certain structural types of compounds, although exceptions may be found.

Because of the discovery of small peaks characteristic of the pyrochlore structure in the X-ray diffraction powder patterns of $\text{La}_2\text{O}_3 \cdot 2\text{ZrO}_2$ and $\text{Nd}_2\text{O}_3 \cdot 2\text{ZrO}_2$, these compositions have been called pyrochlore-type compounds. The presence of these compounds necessitates a revision of the published phase diagrams for these systems, and such revisions have been shown.

6. References

- [1] W. R. Cook and H. Jaffe, *Phys. Rev.* **88**, 1426 (1952).
- [2] W. R. Cook and H. Jaffe, *Phys. Rev.* **89**, 1297 (1953).
- [3] A. Bystrom, *Arkiv Kemi, Mineral. Geol. [A]* **18** (1945).
- [4] L. W. Coughanour, R. S. Roth, S. Marzullo, and F. E. Sennett, *J. Research NBS* **54**, 191 (1955) RP2580.
- [5] N. N. Padrow and C. Schusterius, *Ber. deut. keram. Ges.* **31**, 391 (1954).
- [6] W. H. Davenport, S. S. Kistler, W. N. Wheildon, and O. T. Whittmore, *J. Am. Ceram. Soc.* **33**, 333 (1950).
- [7] H. R. Gaertner, *Jahrb. Min. Beil. Bd. [1]* **61**, (1930).
- [8] O. Rosen and A. Westgren, *Geol. Fören. Förh.* **60**, 226 (1938).
- [9] *International tables for X-ray crystallography*, vol. 1. (Kynoch Press, Birmingham, England, 1952).
- [10] J. Green, *Bul. Geol. Soc. Am.* **64**, 1001 (1953).
- [11] E. A. Wood, *Acta Cryst.* **4**, 353 (1951).
- [12] M. L. Keith and R. Roy, *Am. Mineralogist* **39**, 1 (1954).
- [13] W. Coffeen, *J. Am. Ceram. Soc.* **36**, 207 (1953).
- [14] W. Coffeen (personal communication).
- [15] B. Aurivillius, *Ark. Kem. Sverige.* **1**, 499 (1950).
- [16] S. Roberts, *Phys. Rev.* **76**, 1217 (1949).
- [17] F. H. Brown, Jr. and P. Duwez, *J. Am. Ceram. Soc.* **38**, 95 (1955).
- [18] F. Trombe and M. Foex, *Compt. rend.* **233**, 254 (1951).
- [19] O. Ruff, and F. Ebert, *Z. anorg. u. allgem. Chem.* **180**, 19 (1929).
- [20] P. Duwez, F. H. Brown, Jr., and F. Odell, *J. Electrochem. Soc.* **38**, 356 (1951).
- [21] A. Dietzel and H. Tober, *Ber. deut. keram. Ges.* **30**, 71 (1953).
- [22] C. Schusterius and N. N. Padrow, *Ber. deut. keram. Ges.* **30**, 235 (1953).
- [23] S. M. Lang, F. P. Knudsen, R. S. Roth, and C. L. Filmore, *NBS Circular* 568 (1956).

WASHINGTON, September 21, 1955.